Nano Letters

Supporting Information for "Rotational Mobility of Single Molecules Affects Localization Accuracy in Super-Resolution Fluorescence Microscopy"

Matthew D. Lew,[§] Mikael P. Backlund,[§] and W. E. Moerner

[§]Equal contributions

Supporting Figure S1	Image weighting factor $\eta(\theta,\phi)$ for various cone sizes and orientations
Supporting Figure S2	Effect of faster rotational diffusion on image weighting factor, SM PSFs, and lateral shift
Supporting Figure S3	Effect of cone angle on SM PSFs, intensity, and lateral shift
Supporting Figure S4	SM rotational diffusion effects on pixelated 3D PSFs and lateral shifts
Supporting Figure S5	Defocused SM PSFs as a function of cone angle
Supporting Note	Mathematical framework for modeling the rotational mobility of single molecules

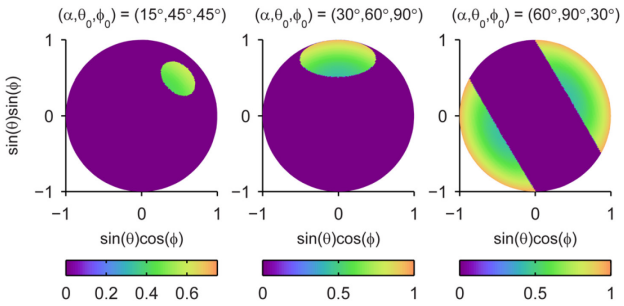

Supporting Figure S1. Image weighting factor $\eta(\theta,\phi)$ for various cone sizes and orientations (α,θ_0,ϕ_0) plotted in two-dimensional orientation space with definitions given by the axes labels. In general, smaller cone angles α yield nearly uniform $\eta(\theta,\phi)$ across the entire cone.

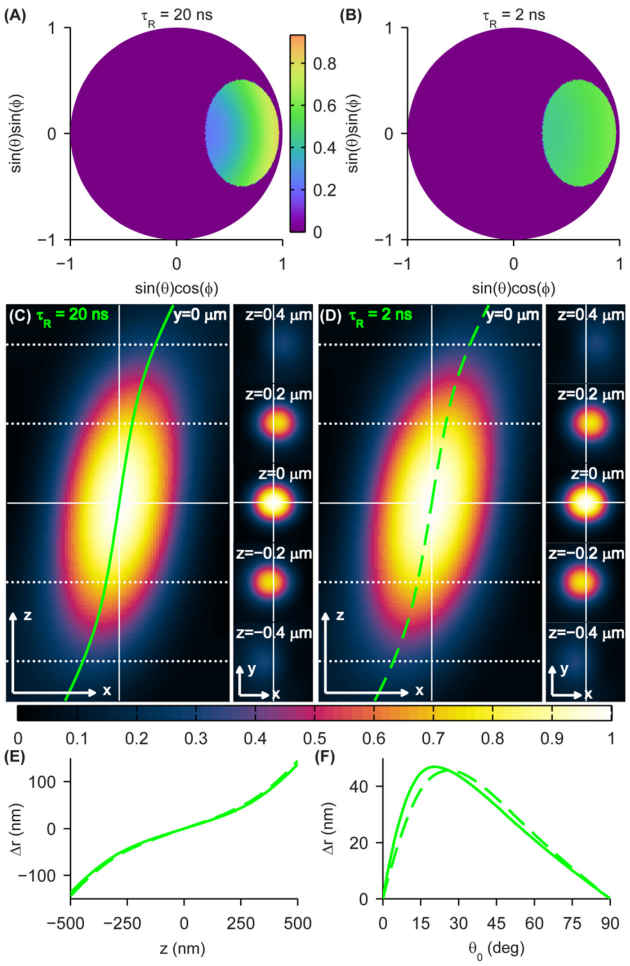

Supporting Figure S2. Effect of faster rotational diffusion on image weighting factor, SM PSFs, and lateral shift. Image weighting factor $\eta(\theta,\phi)$ for $(\alpha,\theta_0,\phi_0) = (30°,45°,0°)$ and rotational correlation times (A) $\tau_R = 20$ ns and (B) $\tau_R = 2$ ns plotted in two-dimensional orientation space with definitions given by the axes labels. (C) *xz* (left) and *xy* (right) cross-sections of the 3D PSF for a SM diffusing within the same cone as above with $\tau_R = 20$ ns. The lateral shift $\Delta r(z)$ is overlaid in green. (B) Same as (A) for a SM diffusing $\tau_R = 2$ ns. The lateral shift $\Delta r(z)$ is overlaid with a dashed green line. The various *z*-planes containing the *xy* cross-sections are denoted by horizontal dotted/solid lines at left. Scale/axes arrows: 200 nm. Lateral shift Δr as a function of (E) axial position z ($\theta_0 = 45°$) and (F) cone axis orientation θ_0 ($z = 200$ nm) for $\tau_R = 20$ ns (solid green) and $\tau_R = 2$ ns (dashed green). The faster correlation time causes the image weighting

factor to be more uniform across the entire cone, but this produces negligible differences in the observed SM PSFs and lateral shifts. The maximum difference in the lateral shift for $\tau_R = 20$ ns and $\tau_R = 2$ ns plotted above is 8 nm, but for most axial positions and orientations, the lateral shift curves are virtually identical.

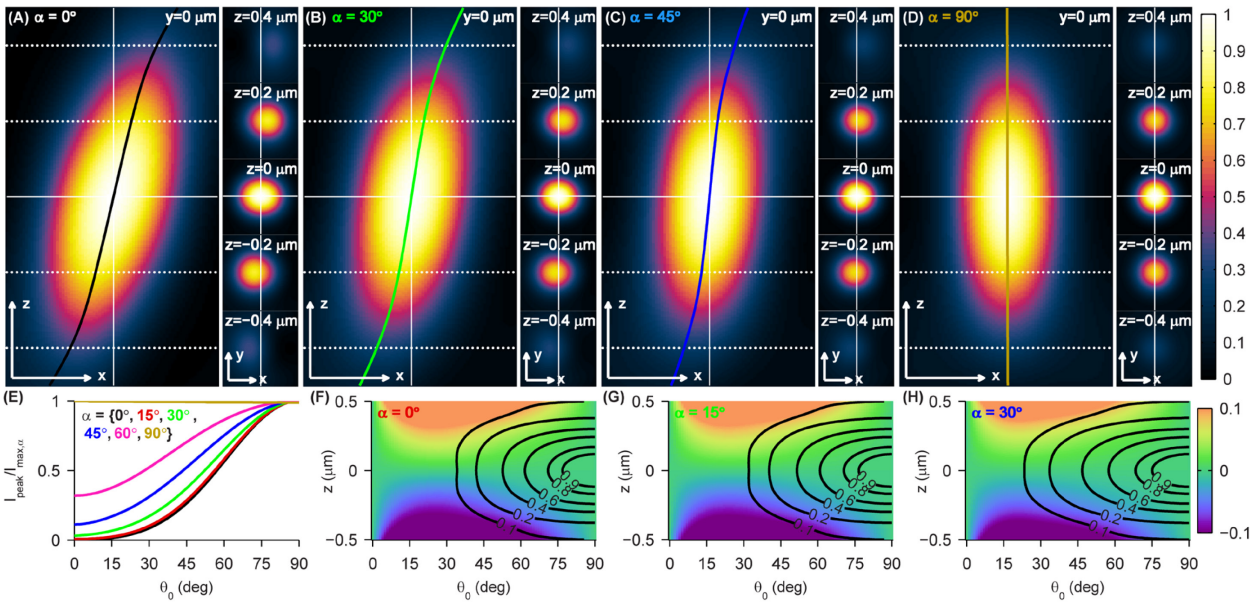

Supporting Figure S3. Effect of cone angle on SM PSFs, intensity, and lateral shift. (A) *xz* (left) and *xy* (right) cross-sections of the 3D PSF for a SM diffusing within the cone (α,θ_0,ϕ_0) = (0°,45°,0°). The lateral shift $\Delta r(z)$ is overlaid in black. (B) Same as (A) for a SM diffusing within the cone (α,θ_0,ϕ_0) = (30°,45°,0°). The lateral shift $\Delta r(z)$ is overlaid in green. (C) Same as (A) for the cone (α,θ_0,ϕ_0) = (45°,45°,0°). The lateral shift $\Delta r(z)$ is overlaid in blue. (D) Same as (A) for the cone (α,θ_0,ϕ_0) = (90°,45°,0°) (free rotational diffusion). The lateral shift $\Delta r(z)$ is overlaid in gold. The various *z*-planes containing the *xy* cross-sections are denoted by horizontal dotted/solid lines at left. Scale/axes arrows: 200 nm. (E) Peak intensity versus orientation plot for cone angles α = {0° (black), 15° (red), 30° (green), 45° (blue), 60° (magenta), 90° (gold)} at constant *z* position. Two-dimensional plots of lateral shift as a function of axial position *z* and orientation θ_0 for (F) α = 0° (fixed dipole), (G) α = 15°, and (H) α = 30°. Color scale is in units of μm and has been saturated to emphasize smaller-scale lateral shifts. The overlaid contours depict the decay in relative intensity for increasing |*z*|/decreasing θ_0. In general, SMs with larger cone angles have smaller lateral shifts and brighter relative intensities compared to those with smaller α for a given

axial position/SM orientation. In addition, molecules with $\Delta r \geq 100$ nm are generally one-tenth as (or less) bright as SMs in focus and oriented perpendicular to the optical axis $\theta_0 = 90°$.

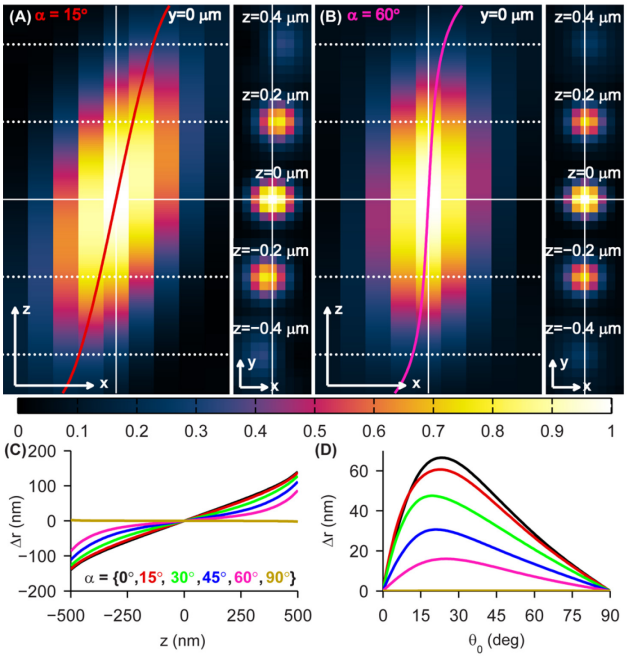

Supporting Figure S4. SM rotational diffusion effects on pixelated 3D PSFs and lateral shifts (65-nm pixel size, see Figure 2 for non-pixelated case). (A) *xz* (left) and *xy* (right) cross-sections of the 3D PSF for a SM diffusing within the cone $(\alpha,\theta_0,\phi_0) = (15°,45°,0°)$. The lateral shift $\Delta r(z)$ is overlaid in red. (B) Same as (A) for a SM diffusing within the cone $(\alpha,\theta_0,\phi_0) = (60°,45°,0°)$. The lateral shift $\Delta r(z)$ is overlaid in magenta. The various *z*-planes containing the *xy* cross-sections are denoted by horizontal dotted/solid lines at left. Scale/axes arrows: 200 nm. (C) Lateral shift Δr as a function of axial position z for $\theta_0 = 45°$ and cone angles $\alpha = \{0°$ (black), 15° (red), 30° (green), 45° (blue), 60° (magenta), 90° (gold)$\}$. (D) Lateral shift Δr as a function of cone axis orientation θ_0 for $z = 0.2$ μm and the same cone angles α as in (C).

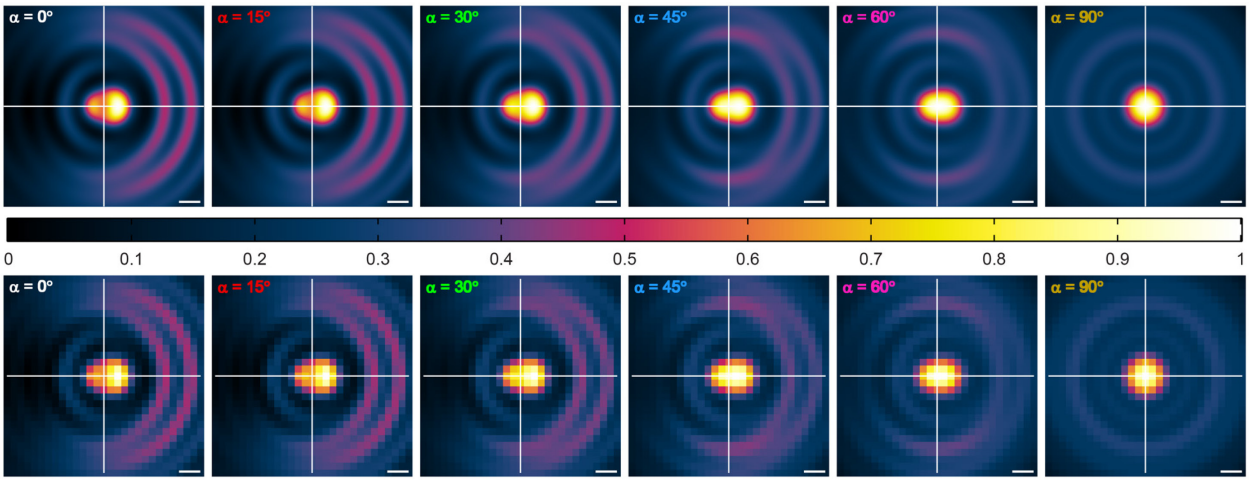

Supporting Figure S5. Defocused SM PSFs as a function of cone angle. The fine features of the defocused SM PSFs ($z = 1$ μm, $\theta_0 = 45°$, $\phi_0 = 0°$) vary subtly as cone angle α increases in both the non-pixelated images (top) and pixelated images (bottom, pixel size = 65 nm in object space). Scale bars: 200 nm.

Supporting Note: Mathematical framework for modeling the rotational mobility of single molecules

A coordinate transformation simplifies the limits of integration of equation 1. The application of the rotation matrix **R** given in S1 converts from the Cartesian basis

$[x, y, z]^T = [\sin\theta\cos\phi, \sin\theta\sin\phi, \cos\phi]^T$ to the rotated basis

$[\tilde{x}, \tilde{y}, \tilde{z}]^T = [\sin\tilde{\theta}\cos\tilde{\phi}, \sin\tilde{\theta}\sin\tilde{\phi}, \cos\tilde{\phi}]^T$.

$$R = \begin{bmatrix} \cos\theta_0\cos\phi_0 & \cos\theta_0\sin\phi_0 & -\sin\theta_0 \\ -\sin\phi_0 & \cos\phi_0 & 0 \\ \sin\theta_0\cos\phi_0 & \sin\theta_0\sin\phi_0 & \cos\theta_0 \end{bmatrix} \tag{S1}$$

This leads to the following definitions for $(\tilde{\theta}, \tilde{\phi})$:

$$\tilde{\theta} = \arccos[\sin\theta_0\sin\theta\cos(\phi - \phi_0) + \cos\theta_0\cos\theta] \tag{S2A}$$

$$\begin{aligned} \tilde{\phi} = \quad & \text{atan}\,2[\sin\theta\sin(\phi - \phi_0), \\ & \cos\theta_0\sin\theta\cos(\phi - \phi_0) - \sin\theta_0\cos\theta] \end{aligned} \tag{S2B}$$

where `atan2(y,x)` refers to the four-quadrant inverse tangent function whose range is [-π,π] (in contrast to the standard `arctan(y/x)` function whose range is [-π/2,π/2]). In these rotated coordinates the integral in equation 1 transforms to:

$$\bar{I}(\alpha, \theta_0, \phi_0) = \int_0^{\alpha} d\tilde{\theta}\sin\tilde{\theta}\int_{-\pi}^{\pi} d\tilde{\phi}\tilde{\eta}(\tilde{\theta}, \tilde{\phi})I[\theta(\tilde{\theta}, \tilde{\phi}), \phi(\tilde{\theta}, \tilde{\phi})], \tag{S3}$$

where we have defined a new weighting factor $\tilde{\eta}(\tilde{\theta}, \tilde{\phi}) = \eta[\theta(\tilde{\theta}, \tilde{\phi}), \phi(\tilde{\theta}, \tilde{\phi}),]$. In evaluating S3 we make use of the inverse relations of S2:

$$\theta = \arccos[\cos\tilde{\theta}\cos\theta_0 - \sin\tilde{\theta}\sin\theta_0\cos\tilde{\phi}] \tag{S5A}$$

$$\begin{aligned} \phi = \quad & \text{atan}\,2[\sin\tilde{\theta}(\cos\tilde{\phi}\sin\phi_0\cos\theta_0 + \sin\tilde{\phi}\cos\phi_0) + \cos\tilde{\theta}\sin\phi_0\sin\theta_0, \\ & \sin\tilde{\theta}(\cos\tilde{\phi}\cos\phi_0\cos\theta_0 - \sin\tilde{\phi}\sin\phi_0) + \cos\tilde{\theta}\cos\phi_0\sin\theta_0] \end{aligned} \tag{S5B}$$

The weighting factor $\tilde{\eta}(\tilde{\theta},\tilde{\phi})$ is the probability density of emitting a photon at orientation $(\tilde{\theta},\tilde{\phi})$, and is given by equation S5.

$$\tilde{\eta}(\tilde{\theta},\tilde{\phi}) = \int_0^{\infty} dt \int_0^{\alpha} d\tilde{\theta}' \sin\tilde{\theta}' \int_{-\pi}^{\pi} d\tilde{\phi}' f(t) g(\tilde{\theta},\tilde{\phi},t \mid \tilde{\theta}',\tilde{\phi}',0) \mid \vec{\mu}(\tilde{\theta}',\tilde{\phi}') \cdot \vec{E}_{inc} \mid^2 \tag{S5}$$

An implicit assumption in equation S5 is that if the molecule is rotationally immobile, its absorption dipole moment is parallel to its emission dipole moment. This assumption is justified by the fact that these two moments are collinear[1] or nearly collinear[2] for many common fluorophores. As discussed in the text, $f(t) = e^{-t/\tau_F} / \tau_F$ is the PDF of emitting a photon a time *t* after absorption. $| \vec{\mu}(\tilde{\theta}',\tilde{\phi}') \cdot \vec{E}_{inc} |^2$ is the PDF of the SM absorbing a photon at orientation $(\tilde{\theta}',\tilde{\phi}')$ (pre-factor containing physical constants omitted), where $\vec{\mu}$ is the absorption dipole and $\vec{E}_{inc}$ is the incident electric field. $g(\tilde{\theta},\tilde{\phi},t \mid \tilde{\theta}',\tilde{\phi}',0)$ is the conditional PDF of the SM having rotated to $(\tilde{\theta},\tilde{\phi})$ at time *t*, given that it was at $(\tilde{\theta}',\tilde{\phi}')$ at time 0. Within the cone, *g* is a solution to the rotational diffusion equation[3] given by

$$\frac{\partial g}{\partial t} = D_{rot}\left[\frac{1}{\sin\tilde{\theta}}\frac{\partial}{\partial\tilde{\theta}}\left(\sin\tilde{\theta}\frac{\partial}{\partial\tilde{\theta}}\right) + \frac{1}{\sin^2\tilde{\theta}}\frac{\partial^2}{\partial^2\tilde{\phi}}\right] g\,, \tag{S6}$$

subject to the boundary condition

$$\left.\frac{\partial g}{\partial\tilde{\theta}}\right|_{\alpha} = 0 \tag{S7}$$

and initial condition

$$g(t=0) = \delta(\tilde{\theta}-\tilde{\theta}')\delta(\tilde{\phi}-\tilde{\phi}')\,. \tag{S8}$$

In equation S6, D_{rot} is the rotational diffusion constant and the bracketed portion is the Laplacian expressed in spherical polar coordinates. The analytical solution[4] is

$$g(\tilde{\theta},\tilde{\phi},t\,|\,\tilde{\theta}',\tilde{\phi}',0)=\sum_{k=1}^{\infty}\sum_{m=0}^{\infty}\mathrm{e}^{-D_{rot}\nu_{km}(\nu_{km}+1)t}[A_{km}P_{\nu_{km}}^{m}(\cos\tilde{\theta})\cos m\tilde{\phi}+B_{km}P_{\nu_{km}}^{m}(\cos\tilde{\theta})\sin m\tilde{\phi}] \tag{S9}$$

where $P_{\nu_{km}}^{m}(\cdot)$ are the Legendre polynomials of non-integer order and the coefficients A_{km} and B_{km} are given by

$$A_{km}=\frac{P_{\nu_{km}}^{m}(\cos\tilde{\phi}')\cos m\tilde{\phi}'}{\pi H_{km}\epsilon_{km}},\qquad \epsilon_{km}=\begin{cases}2 & m=0\\ 1 & m\neq 0\end{cases} \tag{S10A}$$

$$B_{km}=\frac{P_{\nu_{km}}^{m}(\cos\tilde{\phi}')\sin m\tilde{\phi}'}{\pi H_{km}} \tag{S10B}$$

where

$$H_{km}=\int_{0}^{\alpha}d\theta\sin\theta[P_{\nu_{km}}^{m}(\cos\theta)]^{2} \tag{S11}$$

The generally non-integer values of ν_{km} in equation S8 are determined by finding the solutions of the equation

$$P_{\nu_{km}}^{m+1}(\cos\alpha)+m\cot\alpha P_{\nu_{km}}^{m}(\cos\alpha)=0\,. \tag{S12}$$

While the MATLAB function `legendre` computes the associated Legendre functions of integer order, MATLAB does not have a built-in function for evaluating Legendre functions of non-integer order. Thus, we wrote our own routine based on the relationship between these functions and Gauss's hypergeometric function.[4] We wrote custom MATLAB routines to find ν_{km}'s via equation S12 for each $\alpha\in\{15^{\circ},30^{\circ},45^{\circ},60^{\circ}\}$ and calculated the corresponding A_{km} and B_{km} coefficients via equation S9; for the special case of $\alpha = 90°$, $\nu_{km}\in\{0,2,4,...\}$. In our computation of S5 we found it convenient to take advantage of the fact that g is symmetric with respect to $(\tilde{\theta},\tilde{\phi})$ and $(\tilde{\theta}',\tilde{\phi}')$, i.e. $g(\tilde{\theta},\tilde{\phi},t\,|\,\tilde{\theta}',\tilde{\phi}',0)=g(\tilde{\theta}',\tilde{\phi}',t\,|\,\tilde{\theta},\tilde{\phi},0)$. We define the function $\xi(\tilde{\theta}',\tilde{\phi}';\tilde{\theta},\tilde{\phi})$:

(S13)

$$\begin{aligned}
\xi(\tilde{\theta}',\tilde{\phi}';\tilde{\theta},\tilde{\phi}) &= \sin\tilde{\theta}'\int_0^\infty dt f(t) g(\tilde{\theta}',\tilde{\phi}',t\,|\,\tilde{\theta},\tilde{\phi},0) \\
&= \sin\tilde{\theta}'\int_0^\infty dt\left(\frac{1}{\tau_F}e^{-t/\tau_F}\sum_{k=1}^{\infty}\sum_{m=0}^{\infty}\mathrm{e}^{-D_{rot}\nu_{km}(\nu_{km}+1)t}[A_{km}P_{\nu_{km}}^{m}(\cos\tilde{\theta}')\cos m\tilde{\phi}' + B_{km}P_{\nu_{km}}^{m}(\cos\tilde{\theta}')\sin m\tilde{\phi}']\right) \\
&= \sum_{k=1}^{\infty}\sum_{m=0}^{\infty}\left[\frac{1}{\tau_F}\int_0^\infty dt\,\mathrm{e}^{-\{D_{rot}\nu_{km}(\nu_{km}+1)+1/\tau_F\}t}\right][A_{km}P_{\nu_{km}}^{m}(\cos\tilde{\theta}')\cos m\tilde{\phi}' + B_{km}P_{\nu_{km}}^{m}(\cos\tilde{\theta}')\sin m\tilde{\phi}']\sin\tilde{\theta}' \\
&= \sum_{k=1}^{\infty}\sum_{m=0}^{\infty}\left[\frac{1}{\tau_F D_{rot}\nu_{km}(\nu_{km}+1)+1}\right][A_{km}P_{\nu_{km}}^{m}(\cos\tilde{\theta}')\cos m\tilde{\phi}' + B_{km}P_{\nu_{km}}^{m}(\cos\tilde{\theta}')\sin m\tilde{\phi}']\sin\tilde{\theta}'
\end{aligned}$$

such that S5 becomes

$$\tilde{\eta}(\tilde{\theta},\tilde{\phi}) = \int_0^\alpha d\tilde{\theta}'\int_{-\pi}^{\pi} d\tilde{\phi}'\,\xi(\tilde{\theta}',\tilde{\phi}';\tilde{\theta},\tilde{\phi})\,|\,\vec{\mu}(\tilde{\theta}',\tilde{\phi}')\cdot\vec{E}_{inc}\,|^2 \qquad \text{(S14)}$$

The Jacobian $\sin\tilde{\theta}'$ was included in ξ to facilitate convergence in the calculation of ξ described below. We used a custom MATLAB routine to compute ξ for each α and an array of $(\tilde{\theta}',\tilde{\phi}')$ (with 0.25° spacing) and $(\tilde{\theta},\tilde{\phi})$ (with 0.5° spacing). Computation of ξ varied for different α and typically required 2-30 min to calculate ξ over the full range of $(\tilde{\theta}',\tilde{\phi}')$ for each $(\tilde{\theta},\tilde{\phi})$ on an Intel Core 2 Duo 3 GHz workstation. Since $\xi(\tilde{\theta}',\tilde{\phi}'+\delta;\tilde{\theta},\tilde{\phi}+\delta) = \xi(\tilde{\theta}',\tilde{\phi}';\tilde{\theta},\tilde{\phi})$ for all phase shifts δ, it was only necessary to compute ξ directly over a range of $(\tilde{\theta},\tilde{\phi}=0^\circ)$ and then shift the results accordingly. These results were used to evaluate equation S14 and in turn equation S3. The numerical integration of equation S3 was also performed in MATLAB with spacing $d\tilde{\theta} = 0.5°$ for $\alpha \le 90°$ ($d\tilde{\theta} = 1°$ for $\alpha = 90°$) and $d\tilde{\phi} = 6°$.

References

1. Volkmer, A.; Subramanian, V.; Birch, D.; Jovin, T. *Biophys. J.* **2000***, 78,* 1589-1598.

2. Ha, T.; Laurence, T. A.; Chemla, D. S.; Weiss, S. *J. Phys. Chem. B* **1999***, 103,* 6839-6850.

3. Kinosita Jr., K.; Kawato, S.; Ikegami, A. *Biophys. J.* **1977***, 20,* 289-305.

4. Warchol, M. P.; Vaughan, W. E. *Advances in Molecular Relaxation and Interaction Processes* **1978***, 13,* 317-330.